

THE EFFECT OF COMPLEX NUCLEATING AGENT ON THE PHYSICAL AND CHEMICAL PROPERTIES OF $\text{Li}_2\text{O-Al}_2\text{O}_3\text{-SiO}_2$ GLASS CERAMIC

M. Rezvani*

* M_Rezvani@tabrizu.ac.ir

Received: April 2010

Accepted: November 2010

Department of Materials Engineering, Faculty of Mechanical Engineering, University of Tabriz, Tabriz, Iran

Abstract: In the present work, effect of the nucleating agent such as TiO_2 , ZrO_2 , P_2O_5 , Y_2O_3 and CeO_2 in single, double, triple and fourth systems on the crystallization behavior of various compositions was studied. Using differential thermal analysis (DTA), the composition of $\text{Li}_2\text{O-Al}_2\text{O}_3\text{-SiO}_2$ (LAS) was optimized and the coefficient of thermal expansion (CTE), three point flexural strength, hardness, thermal shock resistance, and chemical resistance of the most favorable composition were evaluated. The crystalline phase was determined by the x-ray diffractometry. Moreover, the micro-structure of the samples was studied by SEM technique. According to the results, β -Eucryptites (high quartz solid solution) was the main crystalline phase and the CTE values of the optimized sample were determined as $1.65\text{-}1.93 \times 10^{-6}$ in the temperature range of $20\text{-}500^\circ\text{C}$. Furthermore, three point bending strength ranged from 139 to 155 MPa.

Keyword: Glass, LAS Glass Ceramic, Eucryptite, Low Thermal Expansion.

1. INTRODUCTION

Glass-ceramic materials are produced via the controlled crystallization of glass [1]. The physical and chemical properties of glass-ceramics strongly depend on the composition of glass, type and amount of the crystalline phase, nucleating agents, microstructure, and, finally, the heat treatment procedure [2]. Due to the low thermal expansion, LAS glass-ceramic systems are known for their thermal shock resistance [3-5]. The most effective nuclei in the LAS glass-ceramic system are TiO_2 , ZrO_2 , P_2O_5 , TaO_5 , Y_2O_3 , and CeO_2 [6-24]. Hsu and Speyer, [19] investigations showed that TiO_2 is a more effective nucleating agent than Ta_2O_5 . Hu et al. [18] introduced CeO_2 as effective nucleant. According to Guo et al. [22], using P_2O_5 causes phase separation in glass due to the high ionic field strength of P^{+5} , so reduction in glass viscosity and crystallization temperature improves the nucleation and growth process. Arnault et al. [21] showed even in the presence of Mg^{2+} and Zn^{2+} in the LAS glass-ceramic, TiO_2 and ZrO_2 retained their effective role as nucleating agent.

Idris and Khater [25] demonstrated that simultaneous utilization of two nuclei, e.g. TiO_2 and ZrO_2 , will provide the most effective nucleation condition as compared to the individually utilization. In various glass-ceramic systems, glass

crystallization has led to the enhancement of the mechanical properties. Presence of the crystalline phase with stronger atomic bond and higher modulus increases the strength of such glass-ceramic proportional to the volume fraction of precipitated particles. These phases absorb the crack growth energy [26]. The most important stable crystalline phases in the LAS glass ceramic system is Eucryptite ($\text{Li}_2\text{O}.\text{Al}_2\text{O}_3.2\text{SiO}_2$), Spodumene ($\text{Li}_2\text{O}.\text{Al}_2\text{O}_3.4\text{SiO}_2$) and Petalite ($\text{Li}_2\text{O}.\text{Al}_2\text{O}_3.8\text{SiO}_2$), and meta-stable solid solution i.e. B-quartz (high-quartz) and Kitite (tetragonal SiO_2) whose chemical composition is between the stoichiometric composition (Eucryptite) and SiO_2 [24,27]. CTE values of the LAS glass-ceramic were ranged from 1.9 to $2.2 \times 10^{-6} \text{ }^\circ\text{K}^{-1}$ [27], and their hardness is about 550-650 (Kg/mm^2) [28]. Their bending strength is also about 104 to 140 MPa. The LAS glass-ceramics are suitable for cookware container, cook top panel, telescope mirrors, protective panels, windows of combustion furnace (e.g. for wood, coal, oil, gas), and cover panels in front of the open fireplace [29].

2. EXPERIMENTAL PROCEDURE

The glass preliminary composition (S3) is presented in table 1. The nuclei, TiO_2 , ZrO_2 , P_2O_5 , Y_2O_3 , and CeO_2 were added to the sample S3 (in the single, double, triple and four systems)

in various combinations. The raw materials used in the present investigation were reagent grade silica, α -Al₂O₃ (PB-502 Alumina, Martinswerk), K₂CO₃, NaCO₃, Li₂CO₃, ZrO₂, TiO₂, ZnO, Mg(OH)₂, P₂O₅, Y₂O₃, and CeO₂. The mixture of raw materials after mixing thoroughly were transferred to an alumina crucible and melted at 1650 °C for 2 hours in an electric furnace. Afterwards, the melts were cast in pre-heated stainless steel moulds and cooled naturally to the room temperature. In order to investigate the thermal behavior of the glass samples, DTA technique (DTG-60AH Shimadzu) was used where nucleation temperature (T_n), crystallization peak temperature (T_p), and glass transformation temperature (T_g) were determined. The reference material in these experiments was α -Al₂O₃ powders and the heating rate was 10 °C/min. Dilatometric softening points (T_d) and CTE were also measured by a dilatometer (E-402 Netzsch). The optimum nucleation temperature of the glass was determined by the Ray and Day method [30]. The thermal shock resistance range of the optimized samples was determined from 450 to 700 °C; that is, the samples were heated at a chosen temperature and, then, naturally cooled to the

room temperature after taking them out from the furnace. This procedure was repeated for 40 cycles. The average micro-hardness of the polished glass and glass-ceramic was measured by a Vickers micro-hardness tester (Leitz GMBH D-6630 Wetzlar) with an indentation of 50 gf for 30 seconds. The three point bending strength of the glass and glass ceramic was determined using a universal testing machine (Instron Universal Testing 1196), with loading rate of 0.5 mm/min and based on the ASTM C 158-84 standard. Five polished rectangular specimens (40x5x5 mm) were tested for each composition. The bulk density of the samples was also measured by the Archimedes method. The chemical resistance of the polished glasses and glass-ceramic was determined by immersing them into a solution containing 5% NaOH and 5% HCl at 90 °C for 24 hours where the weight loss of the samples was used as a criterion for chemical resistance. In order to determine the phase structure, the heat-treated samples were subjected to XRD analysis (Siemons-D500) using Cu-k α radiation at 20 kV setting and in 2 ranges from 10 °C to 70 °C. Finally, the samples after polishing and etching in 5% HF solution for 30 seconds were coated with a thin film of gold and subjected to microscope examination by a scanning electron microscope (LEO 440i).

3. RESULTS AND DISCUSSION

Table 1 depicts the chemical composition of the various glasses and fig.1 shows the DTA results of the specimens. Selecting the optimized samples was carried out regarding to the sharpest and lowest temperature of the exothermic peaks. It can be seen that the base composition (specimen S₃) was the most promising specimen exhibiting the highest and sharpest DTA peaks with the lowest temperature in these series. Hence, the sample S₃ was selected as the base glass (Sample S). Fig.2 represents DTA curves of the optimized specimens containing single nucleant. In this series, the sample ST₃ (with a TiO₂ wt% of 3) is the best composition. According to Khater and Edris [25] TiO₂ leads to liquid un-mixing which may be referred to as phase separation. For any glass in which the ratio



Fig. 1. DTA curves of the glasses S₁(1), S₂(2), S₃(3), S₄(4), S₅(5) and S₆(6)

Table1. Chemical composition of glasses (weight percents)

S	SiO ₂	Al ₂ O ₃	Li ₂ O	Na ₂ O	K ₂ O	MgO	ZnO	TiO ₂	ZrO ₂	Y ₂ O ₃	P ₂ O ₅	CeO ₂
S ₁	62.4	27.04	5.2	0.6	0.6	2.08	2.08	-	-	-	-	-
S ₂	64.4	25.04	5.2	0.6	0.6	2.08	2.08	-	-	-	-	-
S ₃	66.4	23.04	5.2	0.6	0.6	2.08	2.08	-	-	-	-	-
S ₄	68.4	21.04	5.2	0.6	0.6	2.08	2.08	-	-	-	-	-
S ₅	70.4	19.04	5.2	0.6	0.6	2.08	2.08	-	-	-	-	-
S ₆	72.4	17.04	5.2	0.6	0.6	2.08	2.08	-	-	-	-	-
S ₇	74.4	15.04	5.2	0.6	0.6	2.08	2.08	-	-	-	-	-
S ₈	76.4	13.04	5.2	0.6	0.6	2.08	2.08	-	-	-	-	-
ST ₃	66.4	23.04	5.2	0.6	0.6	2.08	2.08	3	-	-	-	-
SZ ₄	66.4	23.04	5.2	0.6	0.6	2.08	2.08	-	4	-	-	-
SP ₁	66.4	23.04	5.2	0.6	0.6	2.08	2.08	-	-	-	1	-
SY ₁	66.4	23.04	5.2	0.6	0.6	2.08	2.08	-	-	1	-	-
ST ₃ Z ₁	66.4	23.04	5.2	0.6	0.6	2.08	2.08	3	1	-	-	-
ST ₃ Z ₁ Y ₁	66.4	23.04	5.2	0.6	0.6	2.08	2.08	3	1	1	-	-
ST ₃ Z ₁ C ₃	66.4	23.04	5.2	0.6	0.6	2.08	2.08	3	1	-	-	3

of oxygen ions/network forming cat ions is greater than 2, there must be non-bridging oxygen ions. Tendency to creating separated and non-bridging oxygen ions decreases the viscosity

of the melt and increases the crystallizability of the glasses. Regarding TiO₂, the presence of ZrO₂ does not enhance the crystallizability of the glass, but increases the viscosity and activation energy



Fig . 2. DTA curves of the glasses S(1), ST₃ (2), SZ₄ (3), SP₁ (4) and SY₁ (5)



Fig. 3. DTA curves of the glasses ST₃Z₁ (1), ST₃Z₁Y₁ (2) and ST₃Z₁C₃(3)

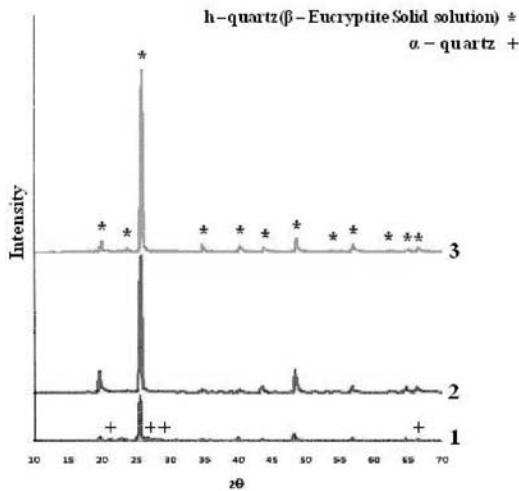


Fig. 4. x-ray diffraction pattern for ST₃Z₁Y₁ (1), ST₃Z₁C₃ (2) and ST₃Z₁ (3) at their DTA peak, crystallization temperature for 3 h.

of crystallization (because of the lower ionic field strength). The specimens containing P₂O₅ exhibit lower crystallization temperature peaks than that of the samples containing ZrO₂. Ionic radius of P⁵⁺ is 0.34 Å (r_{Si⁴⁺ 0.41 Å), since it prefers to form stable tetrahedral network. This tendency limits the ability of glass to be crystallized [31]. The little amount of Y₂O₃ decreases the viscosity and the melting temperature. It was observed through experimentations that CeO₂ can be a very suitable flux; therefore, the obtained melt has higher flow ability than other compositions. According to the DTA curves, CeO₂ cannot act as an effective nucleating agent, while Hue et al [31] introduced CeO₂ as an effective nucleating agent. ZrO₂, P₂O₅, Y₂O₃, and CeO₂ were added to ST₃ (1-4wt%). According to the DTA patterns, TiO₂ along with ZrO₂ as nucleating agents in the S glass composition (sample ST₃) provides more}

appropriate properties. Although the crystallization peak temperature was reduced from 841 °C (ST₃) to 815 °C (ST₃Z₁), increasing the amount of ZrO₂ decreases the crystallization peak intensity. The bulk nucleating rate in the presence of TiO₂ and ZrO₂ additives increased and the uniform crystallization phase was obtained [17]. P₂O₅, Y₂O₃, and CeO₂ were added to ST₃Z₁(1-4Wt.%). According to results shown in fig.3, addition of 1wt% Y₂O₃ (ST₃Z₁Y₁) and 3 wt.% CeO₂ (ST₃Z₁C₃) to the specimen ST₃Z₁ provided better bulk nucleation and crystallization. P₂O₅ and CeO₂ were also added to ST₃Z₁Y₁ and ST₃Z₁C₃ (1-4wt.%). In the both cases crystallization peak temperature increased (above 900 °C) and also did not give rise to the sharpening of DTA exothermic peak. The sharpness of exo-peaks gradually decreased and eventually the peak vanished; therefore, the specimens containing four nucleating agents were not appropriate.

The crystallinity of the base glass and heat-treated glasses was investigated by the X-ray diffractometry. XRD results depicted in Fig.4 reveal the diffraction pattern of the h- quartz (β-eucryptite s.s. JCPDS 70-1580). For the ST₃Z₁Y₁ and ST₃Z₁C₃ specimens, in addition to main phase, the free quartz and h-quartz can be seen. Formation of free quartz causes non-appropriate CTE and thermal shock resistance.

The thermal expansion of the glass ceramic specimens was measured from room temperature to the temperatures of their dilatometric softening points. The results obtained are plotted in fig.5, where ΔL is the change in the original length L. The expansion coefficient (α) was, then, calculated from the equation $\alpha = \Delta L / \Delta T$ where ΔT is the temperature interval over which glass

Table 2. Results of T_g, T_n, T_d and T_p for optimum samples

Sample	T _g (°C)	T _n (°C)	T _d (°C)	T _p (°C)
ST ₃ Z ₁	640	680	671	820
ST ₃ Z ₁ Y ₁	656	694	686	849
ST ₃ Z ₁ C ₃	650	690	680	840

Table 3. Mean and standard deviation of bending strength and micro –hardness, bulk density and CTE of glasses and glass-ceramics

Thermal expansion coefficient (20-600 °C) (°C ⁻¹) 10 ⁻⁶ ×	Density (g/cm ³)		Bending strength (Mpa)		Micro-hardness (kg/mm ²)	Properties Sample
glass-ceramic	glass-ceramic	glass	glass-ceramic	glass		
1.65	2.38	1.95	155 (±8)	85 (±14)	594.1 (±7.09)	ST ₃ Z ₁
1.72	2.28	1.89	145 (±15)	75 (±21)	579.6 (±9.90)	ST ₃ Z ₁ Y ₁
1.93	2.11	1.85	139 (±12)	77 (±25)	532.7 (±2.50)	ST ₃ Z ₁ C ₃

was heated. According to the results, thermal expansion of specimens were almost lower than that of the commercial LAS glass-ceramics (1.9-1.22×10⁻⁶ / °C) [27] due to formation of the h-quartz (-eucryptite s.s) phase. The most suitable nucleation temperature was determined by the Ray and Day method. The samples were first heated for 3 hours at several temperatures, i.e. 600 to 725 °C for ST₃Z₁, 680 to 740 °C for ST₃Z₁Y₁, and 650-740 °C for ST₃Z₁C₃. Then, the DTA test was performed. Table 2 shows the T_g, T_d, T_n (optimum nucleation temperature) and T_p (the crystallization peak temperature of the glasses previously nucleated at their optimum temperature for 3 hours for each glass sample). The optimized glass samples nucleated and crystallized at the optimum temperatures for 3 hours and their thermal shock

resistance, micro-hardness, strength, and chemical resistance (heating rate 10 °C/min) were determined. No thermal shock data is available in the literature, but in this research the samples were heated at 450 °C to 700 °C and naturally cooled to room temperature after taking them out of the furnace. This procedure repeated to 40 cycles. No crack was observed after thermal shock test, so thermal shock resistance was over 650 °C. The thermal shock resistance was reported for the commercial LAS glass-ceramic products such as Ceran (cook top panel), Robax (protective panels and windows), Neoceram (cookware container), and Tempax (pyrex or borosilicate glass) was reported as 700, 650, 450, and 150 °C, respectively [27]. The thermal shock resistance of the optimized samples was higher than that of the cookware glass

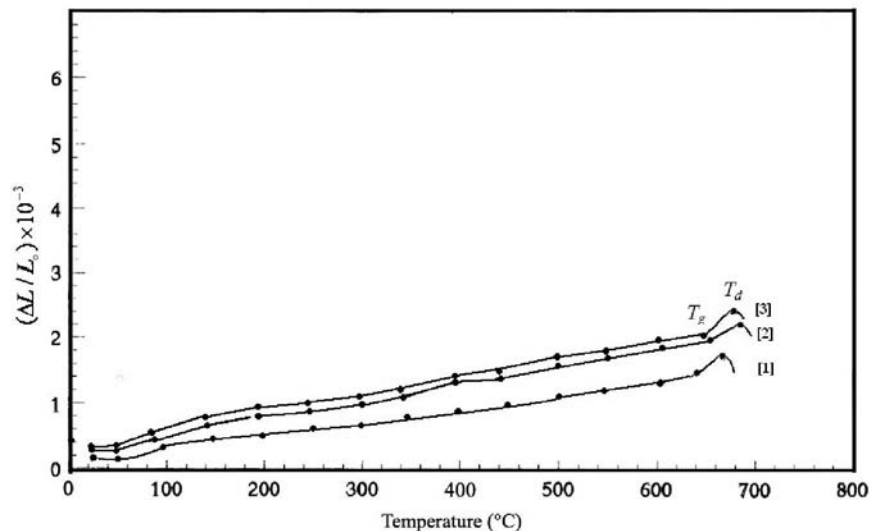
**Fig. 5.** Thermal expansion of ST₃Z₁ (1), ST₃Z₁Y₁ (2) and ST₃Z₁C₃ (3) glass ceramics

Table 4. Chemical resistance of glass-ceramics

Sample	Weight loss in 5%HCl solution (mg.cm ⁻²)	Weight loss in 5%NaOH solution (mg.cm ⁻²)
ST ₃ Z ₁	0.00	0.00
ST ₃ Z ₁ Y ₁	0.01	0.00
ST ₃ Z ₁ C ₃	0.00	0.00

ceramics (the investigated composition in this research was LAS cookware glass-ceramic system).

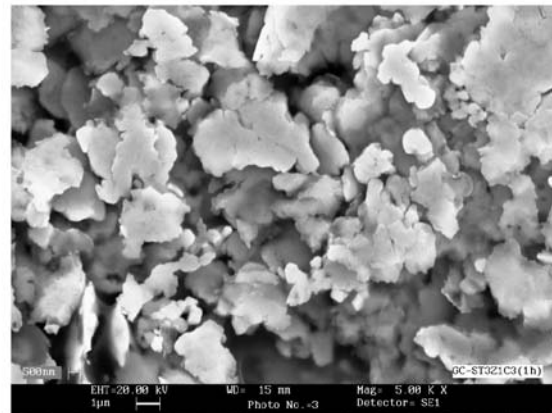
Table 3 shows the three points bending strength, micro-hardness, bulk density, and CTE of various glasses and glass-ceramics. It can be seen that crystallization has led to enhancement of strength of other glasses. The amount, shape, and size of the crystalline phase and porosity are effective parameters which cause variation of the strength of these samples. In early stages of the crystallization, glass viscous flow filled the porosity; however, some of the porosities remained empty after shrinking which are negligible. The bulk density of glass specimens varies between 1.89 to 1.95 g/cm³, whereas in glass ceramics it increased. The bulk density of ST₃Z₁ glass ceramic was about that of the h-quartz (bulk density of -eucryptite s.s is 2.421 g/cm³).The results of glass ceramic ST3Z1 shows higher bending strength (155 MPa) than the mentioned common glass ceramics (104 to 140 MPa).

Fig 6 shows the SEM micrograph of the ST₃Z₁

and ST₃Z₁C₃ glass ceramics nucleated and crystallized at their optimized T_n and T_p for 3 hours. As it can be seen, the precipitated crystalline particles are smaller than 200 nm and ST₃Z₁C₃ particles are bigger than 1 μm. It seems that fine texture of the sample ST₃Z₁ which was fabricated by a suitable nucleating agent led to a high bending strength. The micro-hardness variation of the samples is in a good agreement with their bending strength. As is observed, the ST₃Z₁ glass-ceramic was the hardest sample because of its increased crystallinity and presence of crystals at the surface. Table 4 shows the chemical resistance of the glasses and glass-ceramics. As it is seen, the chemical resistance is higher in the basic environment than acidic environments. In an alkaline environment, glass ceramics show almost no weight loss. The ST₃Z₁ and ST₃Z₁C glass-ceramics exhibit higher chemical resistance. As elucidated earlier, these glass-ceramics can be used as high thermal shock resistance materials for commercial applications where the ST₃Z₁ is the best sample.



(a)



(b)

Fig. 6. SEM micrograph of ST₃Z₁ (a) and ST₃Z₁C₃ (b) nucleated and crystallized at T_n and T_p.

4. CONCLUSION

Simultaneous use of TiO_2 , ZrO_2 , and CeO_2 as nucleating agents with various ratios is a proper approach to obtain a high amount of the crystalline phase in bulk crystallization of glass-ceramics in LAS system. The XRD investigations revealed that the samples consisted of quartz as the minor phase and h-quartz (β -eucryptite s.s.) as the main phase. Nucleation and crystallization temperature of the optimized composition were determined as 680 and 820 °C, respectively. The presence of ZrO_2 and TiO_2 had a significant effect on decreasing the thermal expansion due to the formation of β -eucryptite solid solution (h-quartz) in the optimized samples. The optimized composition (ST_3Z_1) which was nucleated and crystallized at this optimum temperature showed the highest mechanical strength, micro-hardness, and chemical resistance which were much higher than the values reported for $\text{Li}_2\text{O}-\text{Al}_2\text{O}_3-\text{SiO}_2$ system. According to the results, the optimized composition was suitable to be used as a thermal shock resistance material in commercial applications.

REFERENCES

1. Kingery W. D., Bowen H. K. and Uhlmann D. R., Introduction to Ceramics, John Wiley & Son, 1976.
2. Marghussian V. K., Properties and Application of Glass, University of Science and Technology, Tehran, 2002.
3. James P. F., "Glass Ceramic: New Compositions and Uses", J. Non-Crystal Solids, 181: 1-15, 1995.
4. Zawrah M. F., Hamzawy E. M. A. "Effect of Cristobalite Formation on Sinter ability, Microstructure and Properties of Glass/Ceramic Composites", Ceram. Int. 28[2]:123-130, 2002.
5. Tick P. A., Borelli N. F. and Reaney I. M., "The Relationship Between Structure and Transparency in Glass-Ceramic Materials", Opt. Mater. 15: 81, 2000.
6. Kinckerbocker S. and Tuzzolo M. R. "Sinterable β -Spodumene Spodumene Glass-Ceramics", J. Am. Ceram. Soc. 72[10]: 1873-79 (1989).
7. Chatterjee M. and Naska, M. K. "Sol-Gel Synthesis of Lithium Aluminum Silicate Powders: The Effect of Silica Source", Ceram. Int. 32[6]: 623-632, 2006.
8. Wu S. and Liu Y. "Preparation of β -Spodumene Based Glass-Ceramic Powders Polyacrylamid Gel Process", Mat. Lett. 58: 2772-2775, 2004.
9. Strnad Z., Glass Ceramic Materials, Elsevier, New York, 1986.
10. Higashi L. "Kinetics of Crystallization, Phase Transformation and Micro structural Analysis of Corning 9608 glass", Ceram. Int. 23: 471-481, 1997.
11. Barbieri L. and Leonell C. "Nucleation and Crystallization of a Lithium Alumina Silicate Glass", J. Am. Ceram. Soc. 80[12]: 3077-83, 1997.
12. Cheng K., "Determination of Crystallization Kinetic Parameters of $\text{Li}_2\text{O}-\text{Al}_2\text{O}_3-\text{SiO}_2$ Glasses from Derivative Differential Thermal Analysis Curve", Mat. Sci. & Eng. B60: 194-199, 1999.
13. Guedes M. and Ferro A. C. "Nucleation and Crystal Growth in Commercial LAS Compositions", J. Eur. Ceram. Soc. 21:1187-1194, 2001.
14. Rocherulle J. "Nucleation and Growth of a Lithium Aluminum Silicate Glass Studied by DTA", Mat. Reser. Bull. 35: 2353-2361, 2000.
15. Riello P. and Canton P. "Nucleation and Crystallization Behavior of Glass-Ceramic Material in the LAS System of Interest for Their Transparency Properties", J. Non-Crystal Solids. 288: 127-139, 2001.
16. Min H. A and Ming L. K. "Crystallization and Micro structural Changes in Fluorine Containing LAS Glasses", Thermo. Act. 413: 53-55, 2004.
17. Nocun M. and Baugajski W. "Effect of Y-PSZ Additive on the Structure, Thermal Behavior and Mechanical Properties of β -Spodumene Ceramics", Key Eng. Mat. 32[136]: 952-955, 1997.
18. Hu A. M. and Liang K. M. "Phase Transformation of $\text{Li}_2\text{O}-\text{Al}_2\text{O}_3-\text{SiO}_2$ Glasses with CeO_2 Addition", Ceram. Int. 31: 11-14, 2005.
19. Hsu J. and Speyer RF. "Compression of the Effect of Titanium and Tantalum Oxide

- Nucleating Agents on the Crystallization of $\text{Li}_2\text{O-Al}_2\text{O}_3\text{-SiO}_2$ Glasses" , J. Am. Ceram. Soc. 72[12]: 2334-41, 1989.
20. Coon D. N. and Neilson R. N. "Effect of MgO Addition on the Glass Transition Temperature of LAS Glasses", J. Mat. Sci. Lett. 7: 33-35, 1998.
 21. Arnault L. and Gerland M. "Micro structural Study of two LAS-type Glass-Ceramics and Their Parent Glass" , J. Mat. Sci.35: 2331-2345, 2000.
 22. Guo X. and Yang H. "Nucleation and Crystallization Behavior of LAS System Glass-Ceramics Containing Little and no Fluorine", J. Non-Cristal Solids. 351: 2133-2137, 2005.
 23. Cheng K. "Carbon Effect on Crystallization Kinetics of LAS Glasses", J. Non-Cristal Solids . 238:152-157, 1998.
 24. Bach, H. " Low Thermal Expansion Glass-Ceramics", Springer, Berlin, 1995.
 25. Khater G. A. and Idris M.H. "Role of TiO_2 and ZrO_2 on Crystallizing Phases and Microstructure in Li, Ba Aluminosilicate Glass", Ceram. Int.33 [10]:233-238, 2007.
 26. Deriano S., Jerry A., Rouxel T., Sangleboeuf J. C. and Hampshire S., "the Indentation Fracture Toughness (K_c) and its Parameters: the Case of Silica- Rich Glasses" , J. Non-Cristal Solids. 344: 44-50, 2004.
 27. Strnad Z., "Glass Ceramic Materials" , Elsevier, 1986.
 28. Holand W. and Beau G., "Glass-Ceramics Technology ", The American Ceramic Society, Westeilla, 2002.
 29. Scheidler H. and Odeck E., " $\text{Li}_2\text{O-Al}_2\text{O}_3$ Glass-Ceramics", Am. Ceram. Soc. Bull. 68 [11] 1926- 30 , 1989.
 30. Ray C. S. and Day D. E., "New Method for Determining the Nucleation and Crystal-Growth Rates in Glasses", J .Am. Ceram. Soc. 83 [4]:865-72, 2000.
 31. Hu A. M., Liang K. M, Li M. and Mao D. L., "Effect of Nucleation Temperatures and Time on Crystallization Behavior and Properties of $\text{Li}_2\text{O-Al}_2\text{O}_3\text{-SiO}_2$ Glasses", Materials Chemistry and Physics,98:430-433, 2006.